

Original Article

Synthesis, Spectroscopy and Electrochemistry of nitroso terpyridine- {1-(alkyl)-2-(arylo)imidazole}ruthenium(II) Complexes

Prithwiraj Byabartta

Departamento de Quimica Inorganica-Instituto de Ciencia de Materiales de Aragon, Universidad de Zaragoza-CSIC, Zaragoza-50009, Spain

ARTICLE INFO

Corresponding Author:

Prithwiraj Byabartta
pribatta@rediffmail.com

How to cite this article:

El hag A.M.M.A., I. Bushara, A.A. hassabo, I.Y.Turki, and M.O. Eisa. 2014. Synthesis, Spectroscopy and Electrochemistry of nitroso terpyridine-{1-(alkyl)-2-(arylo)imidazole}ruthenium(II) Complexes. *The Journal of Applied Sciences Research*. 1(1): 1-14.

Article History:

Received: 15 September 2014
Revised: 1 October 2014
Accepted: 3 October 2014

ABSTRACT

Silver assisted aqution of blue $[\text{RuCl}(\text{tpy})(\text{RaaiR}^{\prime})](\text{ClO}_4)$ (**1a-1i**) leads to the synthesis of solvento species, blue-violet $[\text{Ru}(\text{OH}_2)(\text{tpy})(\text{RaaiR}^{\prime})](\text{ClO}_4)$ (**2a-2i**), $[\text{RaaiR}^{\prime} = \text{p-R-C}_6\text{H}_5\text{-N}=\text{N-C}_3\text{H}_2\text{-NN}$, abbreviated as N,N'-chelator, R = Me, Et, Bz, p-R=H Me, Cl] that have been reacted with NaNO_2 in warm EtOH resulting in violet nitro complexes of the type, $[\text{Ru}(\text{NO}_2)(\text{tpy})(\text{RaaiR}^{\prime})](\text{ClO}_4)$ (**3a-3i**). The nitrite complexes are useful synthons of electrophilic nitrosyls, and on triturating the nitro compounds with conc. HClO_4 nitrosyl derivatives, $[\text{Ru}(\text{NO})(\text{tpy})(\text{RaaiR}^{\prime})](\text{ClO}_4)_3$ are isolated. The diazotization of the primary aromatic amines with a strongly electrophilic mononitrosyl complex in acetonitrile and dichloromethane solution was thoroughly studied.

Keywords: 1-(alkyl)-2-(arylo)imidazole, nitro, nitroso, ruthenium, amines, MLCT, NMR, CV, IR, reactivity.

Copyright © 2014, World Science and Research Publishing. All rights reserved.

INTRODUCTION

Ruthenium is a component of mixed-metal oxide (MMO) anodes used for cathodic protection of underground and submerged structures, and for electrolytic cells for chemical processes such as generating chlorine from salt water. The fluorescence of some ruthenium complexes is quenched by oxygen, which has led to their use as optode sensors for oxygen. Ruthenium red, $[(\text{NH}_3)_5\text{Ru-O-Ru}(\text{NH}_3)_4\text{-O-Ru}(\text{NH}_3)_5]^{6+}$, is a biological stain used to stain polyanionic molecules such as pectin and nucleic acids for light microscopy and electron microscopy (Atsushi *et al.*, 2014 ; Anna Rathgeb *et al.*; 2014; Sarat Chandra Patra *et al.*; 2014, Stephan Sinn *et al.*; 2014, Stephan Sinn *et al.*; 2014). The beta-decaying isotope 106 of ruthenium is used in radiotherapy of eye tumors, mainly malignant melanomas of the uvea. Ruthenium-centered complexes are being researched for possible anticancer properties. Compared with platinum complexes, those of ruthenium show greater resistance to hydrolysis

and more selective action on tumors. NAMI-A and KP1019 are two drugs undergoing clinical evaluation against metastatic tumors and colon cancers. Because of its ability to harden platinum and palladium, ruthenium is used in platinum and palladium alloys to make wear-resistant electrical contacts. In this application, only thin plated films are used to achieve the necessary wear-resistance (Justin Neill *et al.*; 2008;); Maria Abrahamsson *et al.*, 2008 ; Fábio G. Doro *et al.*, 2008; Wai-Man Cheung *et al.*, 2008; Konstantinos Gkionis *et al.*, 2008; Seann P. Mulcahy *et al.*, 2008 (Communication), Aaron Staniszewski *et al.*, 2008 (Communication), Ali H. Younes *et al.*, 2008; Devis Di Tommaso *et al.*, 2008; James K. Hurst *et al.*, 2008). Because of its lower cost and similar properties compared to rhodium, the use as plating material for electric contacts is one of the major applications. The thin coatings are either applied by electroplating or sputtering. Ruthenium dioxide and lead and bismuth ruthenates are used in thick-film chip resistors. These two electronic applications account for 50% of the ruthenium consumption. Only a few ruthenium alloys are used other than those with other platinum group metals. Ruthenium is often used in small quantities in those alloys to improve some of their properties. The beneficial effect on the corrosion resistance of titanium alloys led to the development of a special alloy containing 0.1% ruthenium. Ruthenium is also used in some advanced high-temperature single-crystal superalloys, with applications including the turbine blades in jet engines. Several nickel based superalloy compositions are described in the literature. Among them are EPM-102 (with 3% Ru) and TMS-162 (with 6% Ru), as well as TMS-138 and TMS-174 both containing 6% rhenium. Fountain pen nibs are frequently tipped with alloys containing ruthenium. From 1944 onward, the famous Parker 51 fountain pen was fitted with the "RU" nib, a 14K gold nib tipped with 96.2% ruthenium and 3.8% iridium.

Now, nitric oxide (NO) has been the focus of discussion because of the discovery of its role in immune defense mechanisms, neuronal signaling processes, cardiovascular systems and in environmental chemistry (Robert Staehle *et al.*, 2014; Amlan K. Pal *et al.*, 2014; Joaquín Alós *et al.*, 2014; Zahra Almodares *et al.*, 2014; Katharine A. Smart *et al.*, 2014; Sumit Saha *et al.*, 2014; Melissa V. Werrett *et al.*, 2013; Christi L. Whittington *et al.*, 2013). The recent observations of the relevance of nitric oxide (NO) in a wide range of biological and environmental processes have led to a resurgence of interest in the area of nitrosyl chemistry. Moreover, the development of metal nitrosyl complexes having a high degree of electrophilic character of the coordinated NO function ($\nu_{\text{NO}} > 1900 \text{ cm}^{-1}$) is a formidable challenge, since the electrophilic NO centre is susceptible to fascinating molecular transformations in contact with nucleophiles. Extensive studies have been made on ruthenium nitrosyls and appreciable variation of the electronic aspect of the NO function attached to the metal centre has been observed depending on the nature of the ancillary groups present. This has prompted me to develop a new class of ruthenium nitrosyl complexes encompassing a combination of strong π -acidic heterochelates. The primary intention is to introduce a high degree of electrophilicity at the nitrosyl centre and subsequently explore the reactivity of this centre to nucleophiles. A new class of ruthenium nitrosyl complexes of the type $[\text{Ru}(\text{tpy})(\text{L})(\text{NO})]$ (tpy = terpyridine; L = azo-imine functionalities) and their precursor nitro complexes $[\text{Ru}(\text{tpy})(\text{L})(\text{NO}_2)]$ have been synthesized. The azoimidazole ligand (L) has selectively been chosen as this in combination with terpyridine has generated highly acidic aqua derivatives (Nathir A. F. Al-Rawashdeh *et al.*, 2013, Rongwei Zhou *et al.*, 2013; Wei Su *et al.*, 2013; Michael R. Norris, *et al.*, 2013; Onduru S. Odongo *et al.*, 2008; Kevin D. Hesp *et al.*, 2008 (Communication), Júlio S. Rebouças *et al.*, 2008; Priti Singh *et al.*, 2008). Consequently the present nitrosyl derivatives $[\text{Ru}(\text{tpy})(\text{L})(\text{NO})]$ exhibit the strongest electrophilic NO centre ($\nu_{\text{NO}} \approx 1960 \text{ cm}^{-1}$) ever reported in ruthenium mononitrosyl chemistry (Susanne Karlsson *et al.*, 2008; Ariadna Garza-Ortiz *et al.*, 2008; Gina L. Fiore *et al.*, 2008; Olof Johansson *et al.*, 2008; Wai-Lun Man *et al.*, 2008; Olivier Hamelin *et al.*, 2008; Ying Cui *et al.*, 2008; Fabienne Alary *et al.*, 2008). Recently, we have developed the arylazoimidazole chemistry of ruthenium and have synthesised chloro, aquo, nitro, nitroso

compounds and tris chelate species reacting with camphor and hydrazone derivatives [L= RaaiR' =p-R-C₆H₅-N=N-C₃H₂-NN, abbreviated as N,N'-chelator, R = Me (**a**), Et (**b**), Bz (**c**), p-R=H, Me, Cl]. The nitrites are useful synthons of nitrosyls, and mononitrosyl compounds are produced in perchloric acid medium. The diazotization of primary amines with the nitroso complexes and after all their coupling product were isolated and also were thoroughly examined.

EXPERIMENTAL

Materials and Physical measurements

Published methods were used to prepare [Ru(OH₂)(tpy)(RaaiR)](ClO₄)₂. All other chemicals and organic solvents used for preparative work were of reagent grade (SRL). The purification of MeCN and preparation of [n-BuN][ClO] respectively used as solvent and supporting electrolyte in electrochemical experiments were done following the literature method. Microanalytical data (C, H, N) were collected using a Perkin Elmer 2400 CHN instrument. Solution electronic spectra were recorded on a JASCO UV-VIS-NIR V-570 spectrophotometer. I.r. spectra were obtained using a JASCO 420 spectrophotometer (using KBr disks, 4000-200 cm⁻¹). The H nmr spectra in CDCl₃ were obtained on a Bruker 500 MHz FT n.m.r spectrometer using SiMe₄ as internal reference. Solution electrical conductivities were measured using a Systronics 304 conductivity meter with solute concentration 10 M in acetonitrile. Electrochemical work was carried out using an EG & G PARC Versastat computer controlled 250 electrochemical system. All experiments were performed under a N₂ atmosphere at 298K using a Pt-disk milli working electrode at a scan rate of 50 mVs⁻¹. All results were referenced to a saturated calomel electrode (SCE).

Preparation of the Complexes

CAUTION ! Perchlorates of heavy metal ions with organic ligands are potentially explosive. Due care must be exercised to avoid explosion hazards. **Preparation of Nitro-{2-(p-tolylazopyrimidine)}-(terpyridine)-ruthenium(II), [Ru(NO₂)(tpy)(RaaiMe)](ClO₄)**

To an EtOH blue-violet solution (15 cm) of [Ru(OH₂)(RaaiMe)(tpy)](ClO₄) (0.1 g, 0.14 mmol) was added 0.019 g (0.27 mmol) of solid NaNO₂, and the mixture was stirred at 343-353 K for 12 h. The violet solution that resulted was concentrated (4 cm) and kept in a refrigerator overnight (12 h). The precipitate was collected by filtration, washed thoroughly with water and dried in vacuo over CaCl₂. Analytically pure dinitro complexes were obtained after chromatography over an alumina (neutral) column on eluting the violet band with toluene-acetonitrile (4:1, v/v) and evaporating slowly in air. The yield was 0.088 g (80%). Analysis for [Ru(O₂N)(HaaiMe)(tpy)](ClO₄), **3a**, Found: C, 45.6, H, 3.3, N, 16.8 Calcd for [C₂₅H₂₁N₈RuO₂](ClO₄), C, 45.1, H, 3.2, N, 16.8; IR(KBr disk, cm⁻¹) ν(NO₂)_{asy} 1300, ν(NO₂)_{sy} 1250, ν(N=N) 1371, ν(C=N), 1575, ESIMS, 665.5[M⁺], 566[M-(ClO₄)]; UV-Vis [λ_{max}(nm)(10⁻³/dm mol cm⁻¹)], 500(8379), 311(28913), 280(26000), 222(50232); Cyclic Voltammetry [E/V (E_p / mV)], 1.33(100), -0.68(90), -0.81(100), -1.36(80). Analysis for [Ru(O₂N)(MeaaiMe)(tpy)](ClO₄), **3b**, Found: C, 45.9, H, 3.4, N, 16.5 Calcd for [C₂₆H₂₃N₈RuO₂](ClO₄), C, 45.1, H, 3.2, N, 16.1; IR(KBr disk, cm⁻¹) ν(NO₂)_{asy} 1300, ν(NO₂)_{sy} 1254, ν(N=N) 1371, ν(C=N), 1585, ESIMS, 679.5[M⁺], 580[M-(ClO₄)]; UV-Vis [λ_{max}(nm)(10⁻³/dm mol cm⁻¹)], 509(8379), 319(27913), 281(24099), 226(56232); Cyclic Voltammetry [E/V (E_p / mV)], 1.39(110), -0.78(90), -0.89(100), -1.39(90). Analysis for [Ru(O₂N)(ClaaiMe)(tpy)](ClO₄), **3c**, Found: C, 42.6, H, 2.8, N, 16.0 Calcd for [C₂₅H₂₀N₈RuClO₂](ClO₄), C, 42.1, H, 2.9, N, 16.8; IR(KBr disk, cm⁻¹) ν(NO₂)_{asy} 1309, ν(NO₂)_{sy} 1259, ν(N=N) 1371, ν(C=N), 1575, ESIMS, 700[M⁺], 600.5[M-(ClO₄)]; UV-Vis

[λ_{\max} (nm)(10⁻³ /dm mol³ cm⁻¹), 503(8079), 319(28913), 289(20000), 229(44232); Cyclic Voltammetry [E/V (E_p / mV)], 1.38(100), -0.61(90), -0.89(100), -1.39(90). Analysis for [Ru(O₂N)(HaaiEt)(tpy)](ClO₄), **3d**, Found: C, 45.6, H, 3.3, N, 16.8 Calcd for [C₂₆H₂₃N₈RuO₂](ClO₄), C, 45.1, H, 3.4, N, 16.8; IR(KBr disk, cm⁻¹) ν (NO₂)_{asy} 1300, ν (NO₂)_{sy} 1258, ν (N=N) 1379, ν (C=N), 1579, ESIMS, 679.5[M⁺], 580[M-(ClO₄)]; UV-Vis [λ_{\max} (nm)(10⁻³ /dm mol³ cm⁻¹), 509(8079), 319(20913), 289(26099), 225(50882); Cyclic Voltammetry [E/V (E_p / mV)], 1.43(100), -0.61(100), -0.89(100), -1.46(100). Analysis for [Ru(O₂N)(MeaaiEt)(tpy)](ClO₄), **3e**, Found: C, 46.6, H, 3.6, N, 16.8 Calcd for [C₂₇H₂₅N₈RuO₂](ClO₄), C, 45.8, H, 3.9, N, 16.1; IR(KBr disk, cm⁻¹) ν (NO₂)_{asy} 1300, ν (NO₂)_{sy} 1259, ν (N=N) 1371, ν (C=N), 1575, ESIMS, 693.5[M⁺], 594[M-(ClO₄)]; UV-Vis [λ_{\max} (nm)(10⁻³ /dm mol³ cm⁻¹), 501(8009), 319(20013), 289(26011), 223(50200); Cyclic Voltammetry [E/V (E_p / mV)], 1.34(100), -0.78(90), -0.89(100), -1.46(100). Analysis for [Ru(O₂N)(ClaaiEt)(tpy)](ClO₄), **3f**, Found: C, 43.6, H, 3.3, N, 15.8 Calcd for [C₂₆H₂₂N₈RuClO₂](ClO₄), C, 43.1, H, 3.2, N, 15.8; IR(KBr disk, cm⁻¹) ν (NO₂)_{asy} 1310, ν (NO₂)_{sy} 1253, ν (N=N) 1379, ν (C=N), 1575, ESIMS, 714[M⁺], 614.5[M-(ClO₄)]; UV-Vis [λ_{\max} (nm)(10⁻³ /dm mol³ cm⁻¹), 500(8379), 311(28913), 280(26000), 222(50232); Cyclic Voltammetry [E/V (E_p / mV)], 1.33(100), -0.68(90), -0.81(100), -1.36(80). Analysis for [Ru(O₂N)(HaaiBz)(tpy)](ClO₄), **3g**, Found: C, 50.6, H, 3.3, N, 15.8 Calcd for [C₃₁H₂₅N₈RuO₂](ClO₄), C, 50.1, H, 3.2, N, 15.1; IR(KBr disk, cm⁻¹) ν (NO₂)_{asy} 1309, ν (NO₂)_{sy} 1259, ν (N=N) 1371, ν (C=N), 1579, ESIMS, 741.5[M⁺], 642[M-(ClO₄)]; UV-Vis [λ_{\max} (nm)(10⁻³ /dm mol³ cm⁻¹), 507(8009), 319(28003), 289(26033), 224(50442); Cyclic Voltammetry [E/V (E_p / mV)], 1.37(100), -0.68(100), -0.84(80), -1.34(80). Analysis for [Ru(O₂N)(MeaaiBz)(tpy)](ClO₄), **3h**, Found: C, 51.6, H, 3.6, N, 15.1 Calcd for [C₃₂H₂₇N₈RuO₂](ClO₄), C, 51.8, H, 3.7, N, 15.0; IR(KBr disk, cm⁻¹) ν (NO₂)_{asy} 1309, ν (NO₂)_{sy} 1259, ν (N=N) 1371, ν (C=N), 1575, ESIMS, 755.5[M⁺], 656[M-(ClO₄)]; UV-Vis [λ_{\max} (nm)(10⁻³ /dm mol³ cm⁻¹), 510(8300), 311(28003), 280(26011), 222(50202); Cyclic Voltammetry [E/V (E_p / mV)], 1.33(80), -0.68(100), -0.81(100), -1.36(80). Analysis for [Ru(O₂N)(ClaaiBz)(tpy)](ClO₄), **3i**, Found: C, 47.6, H, 3.1, N, 14.8 Calcd for [C₃₁H₂₄N₈RuClO₂](ClO₄), C, 47.1, H, 3.2, N, 14.8; IR(KBr disk, cm⁻¹) ν (NO₂)_{asy} 1309, ν (NO₂)_{sy} 1259, ν (N=N) 1371, ν (C=N), 1575, ESIMS, 776[M⁺], 676.5[M-(ClO₄)]; UV-Vis [λ_{\max} (nm)(10⁻³ /dm mol³ cm⁻¹), 506(8009), 319(29013), 280(26333), 227(50232); Cyclic Voltammetry [E/V (E_p / mV)], 1.23(100), -0.78(90), -0.88(80), -1.36(80).

Preparation of [Ru](NO)(HaaiMe)(tpy)](ClO₄)₃ (**4a**)

[Ru(NO₂)(HaaiMe)(tpy)]⁺ (**3a**) (0.1 g, 0.17 mmol) and conc. HClO₄ (3 cm³) were placed in a small beaker, and the mixture was triturated with a glass rod for 1 h. The mixture immediately changed from violet to orange-red. The pasty mass was extracted with CH₂Cl₂ (4 × 5 cm³) and concentrated under reduced pressure. The dark red crystalline product was separated by filtration, washed with chilled H₂O containing a few drops of dil. HClO₄ and dried in vacuo over P₄O₁₀ to yield analytically pure (**4a**), [Yield 0.092 g (70%)]; Analysis for [Ru(ON)(HaaiMe)(tpy)](ClO₄)₃, **4a**, Found: C, 35.6, H, 2.3, N, 13.8 Calcd for [C₂₅H₂₁N₈RuO](ClO₄)₃, C, 35.1, H, 2.2, N, 13.8; IR(KBr disk, cm⁻¹) ν (NO) 1900, ν (ClO₄) 1140, 1100, 1090, 640, 625, ν (N=N) 1371, ν (C=N), 1575, ESIMS, 848.5[M⁺], 550[M-3(ClO₄)]; UV-Vis [λ_{\max} (nm)(10⁻³ /dm mol³ cm⁻¹), 360(8009), 320(10913), 280(14000),

220(30032); Cyclic Voltammetry [E/V (E_p / mV)], 1.7(80), 0.7(90), 0.04, -0.68(90), -0.81(80), -1.3(80). Analysis for [Ru(ON)(MeaiMe)(tpy)](ClO₄)₃, **4b**, Found: C, 36.6, H, 2.7, N, 12.8 Calcd for [C₂₆H₂₃N₈RuO](ClO₄)₃, C, 36.1, H, 2.7, N, 12.8; IR(KBr disk, cm⁻¹) ν (NO) 1909, ν (ClO₄) 1140,1109,1090,649,625, ν (N=N) 1379, ν (C=N), 1575, ESIMS, 862.5[M⁺], 564[M-3(ClO₄)];. Analysis for [Ru(ON)(ClaiMe)(tpy)](ClO₄)₃, **4c**, Found: C, 33.6, H, 2.3, N, 12.8 Calcd for [C₂₅H₂₀N₈RuClO](ClO₄)₃, C, 33.1, H, 2.2, N, 12.8; IR(KBr disk, cm⁻¹) ν (NO) 1900, ν (ClO₄) 1140,1100,1090,640,625, ν (N=N) 1371, ν (C=N), 1575, ESIMS, 883[M⁺], 584.5[M-3(ClO₄)];. Analysis for [Ru(ON)(HaaiEt)(tpy)](ClO₄)₃, **4d**, Found: C, 36.6, H, 2.7, N, 12.8 Calcd for [C₂₆H₂₃N₈RuO](ClO₄)₃, C, 36.1, H, 2.7, N, 12.8; IR(KBr disk, cm⁻¹) ν (NO) 1909, ν (ClO₄) 1140,1109,1099,649,625, ν (N=N) 1371, ν (C=N), 1575, ESIMS, 862.5[M⁺], 564[M-3(ClO₄)];. Analysis for [Ru(ON)(MeaiEt)(tpy)](ClO₄)₃, **4e**, Found: C, 36.6, H, 2.8, N, 12.8 Calcd for [C₂₇H₂₅N₈RuO](ClO₄)₃, C, 36.9, H, 2.8, N, 12.8; IR(KBr disk, cm⁻¹) ν (NO) 1909, ν (ClO₄) 1149,1109,1099,649,625, ν (N=N) 1379, ν (C=N), 1579, ESIMS, 876.5[M⁺], 578[M-3(ClO₄)];. Analysis for [Ru(ON)(ClaiEt)(tpy)](ClO₄)₃, **4f**, Found: C, 34.6, H, 2.5, N, 12.8 Calcd for [C₂₆H₂₂N₈RuClO](ClO₄)₃, C, 34.1, H, 2.5, N, 12.8; IR(KBr disk, cm⁻¹) ν (NO) 1909, ν (ClO₄) 1140,1109,1099,649,625, ν (N=N) 1379, ν (C=N), 1575, ESIMS, 897[M⁺], 598.5[M-3(ClO₄)];. Analysis for [Ru(ON)(HaaiBz)(tpy)](ClO₄)₃, **4g**, Found: C, 39.6, H, 2.7, N, 11.8 Calcd for [C₃₁H₂₅N₈RuO](ClO₄)₃, C, 39.1, H, 2.9, N, 11.8; IR(KBr disk, cm⁻¹) ν (NO) 1902, ν (ClO₄) 1140,1100,1090,640,625, ν (N=N) 1371, ν (C=N), 1575, ESIMS, 934.5[M⁺], 636[M-3(ClO₄)]; Analysis for [Ru(ON)(MeaiBz)(tpy)](ClO₄)₃, **4h**, Found: C, 40.6, H, 2.9, N, 11.8 Calcd for [C₃₂H₂₇N₈RuO](ClO₄)₃, C, 40.9, H, 2.9, N, 11.8; IR(KBr disk, cm⁻¹) ν (NO) 1909, ν (ClO₄) 1149,1109,1099,640,625, ν (N=N) 1379, ν (C=N), 1575, ESIMS, 938.5[M⁺], 640[M-3(ClO₄)];. Analysis for [Ru(ON)(ClaiBz)(tpy)](ClO₄)₃, **4i**, Found: C, 38.6, H, 2.5, N, 11.8 Calcd for [C₃₁H₂₄N₈RuOCl](ClO₄)₃, C, 38.1, H, 2.2, N, 11.8; IR(KBr disk, cm⁻¹) ν (NO) 1909, ν (ClO₄) 1140,1109,1090,649,625, ν (N=N) 1371, ν (C=N), 1575, ESIMS, 959[M⁺], 660.5[M-3(ClO₄)].

Interconversion: [Ru(NO)(RaaiMe)(tpy)](ClO₄)₃ (**4a**) [Ru(NO₂)(RaaiMe)(tpy)] (ClO₄)₃ (**3a**)

To an aqueous solution of (**4a**) (0.1 g, 0.13 mmol) was added an equivalent amount of KOH in the same solvent. The orange-red solution immediately turned violet, and was extracted with CH₂Cl₂. The solvent was removed by evaporation under reduced pressure and the pasty mass, dissolved in a minimum vol. of CH₂Cl₂, was chromatographed on an alumina (neutral) column. A deep violet band was eluted with toluene-acetonitrile (4:1, v/v). The identity of the product as (**3a**) was checked by comparing properties with an authentic sample. The yield was almost quantitative.

Reaction of Primary Amines with [Ru(NO)(RaaiMe)(tpy)](ClO₄)₃

Method (a): To a acetonitrile solution (20 cm) of [Ru(NO)(RaaiMe)(tpy)](ClO₄)₃ (0.2 g, 0.26 mmol) equivalent amounts of aniline (0.054 g, 0.26 mmol) was added, and the mixture was stirred for 30 min at room temperature and then evaporated to dryness using a vacuum pump. The crude pdt was then extracted with 30 cc of ice-cold water and the aqueous solution was collected by filtration. To the aqueous solution an aqueous solution of alkaline b-naphthol was added with continuous stirring over a period of 15 min. Red crystal of 1-phenylazo-2-naphthol were separated and recrystallised from methanol. The residue was dried and dissolved in dichloromethane and brown crystal of [Ru(S)(RaaiMe)(tpy)]ClO₄ (S = CHCN) (**6a**) were obtained.

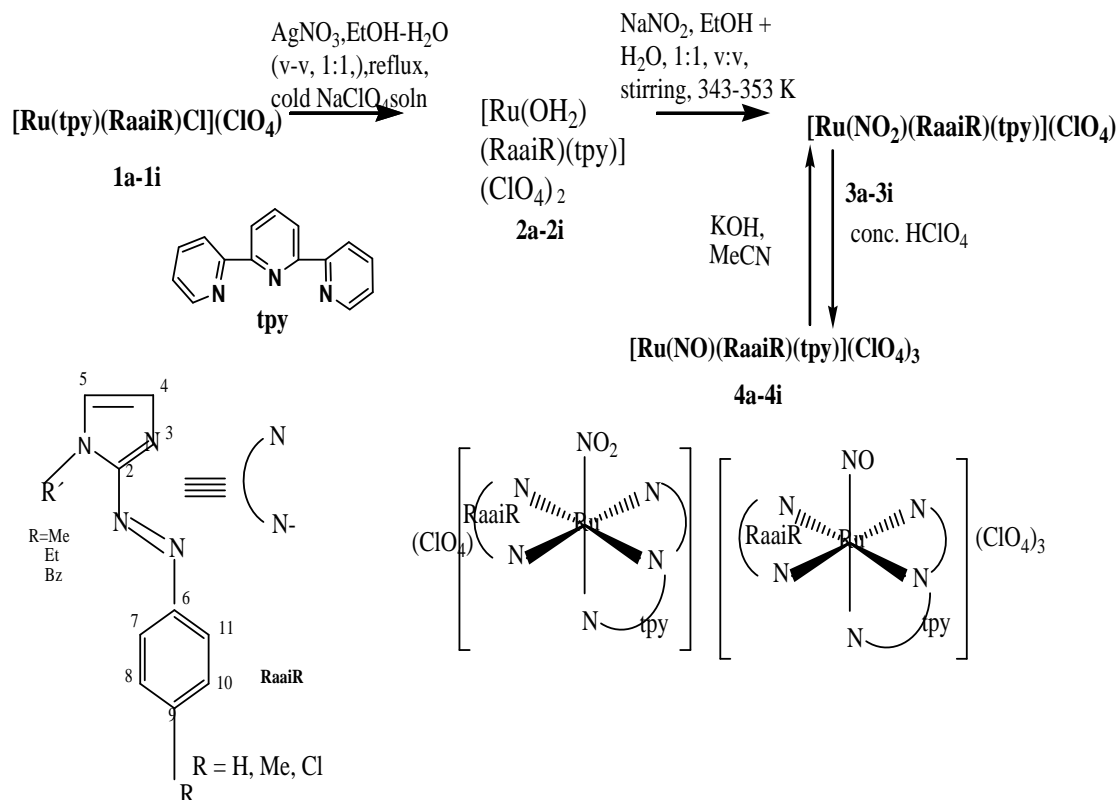
Method (b): To a dichloromethane solution (20 cm) of [Ru(NO)(RaaiMe)(tpy)](ClO₄)₃ (0.2 g, 0.26 mmol) equivalent amounts of aniline (0.054 g, 0.26 mmol) was added and the mixture was stirred for 30 min at room temperature and then evaporated to dryness using a vacuum pump. Brownish white needles of [C₆H₅N][ClO₄] were collected. The residue was

then extracted with 30 cc of ice-cold water and the aqueous solution was collected by filtration. To the aqueous solution an aqueous solution of alkaline *b*-naphthol was added with continuous stirring over a period of 15 min. Red crystal of 1-phenylazo-2-naphthol were separated and recrystallised from methanol. The residue was dried and dissolved in dichloromethane and brown crystal of $[\text{Ru}(\text{S})(\text{RaaiMe})(\text{tpy})](\text{ClO}_4)_2 \cdot \text{H}_2\text{O}$ ($\text{S}=\text{H}_2\text{O}$) (**7a**) were obtained. These were collected by filtration and dried in vacuo over P_4O_{10} .

RESULTS AND DISCUSSION

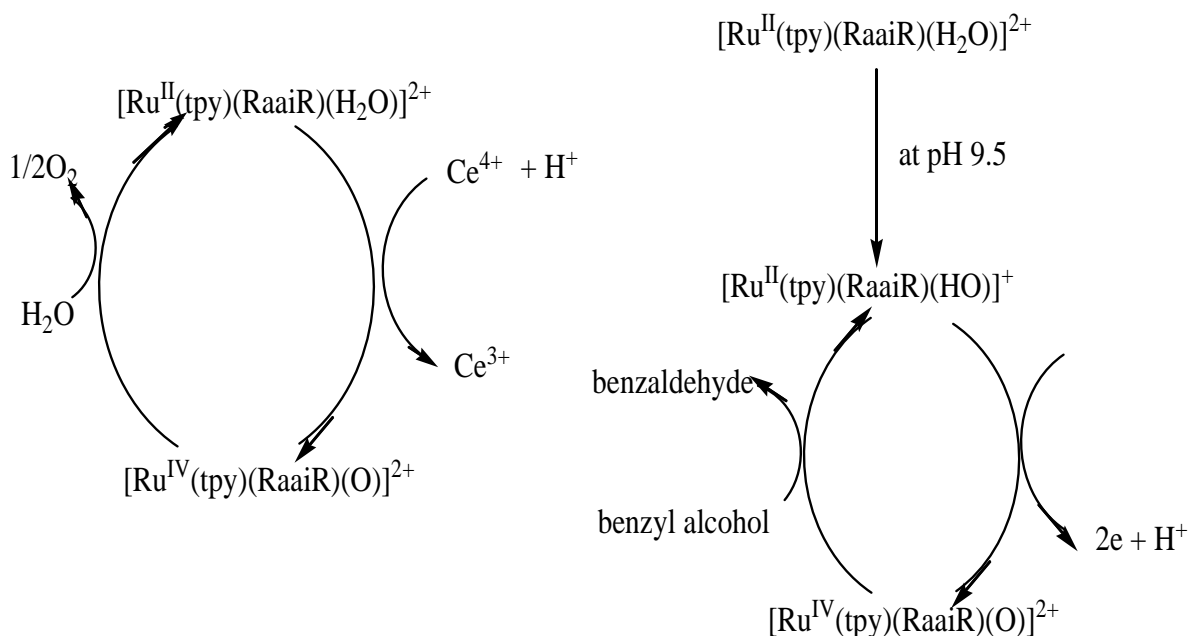
Synthesis and formulation

Aquo complexes $[\text{Ru}(\text{OH}_2)(\text{RaaiR})(\text{tpy})](\text{ClO}_4)_2$, prepared by Ag^+ -assisted aquation of $[\text{RuCl}(\text{RaaiR})(\text{tpy})]^+$ (**1a-1i**), $[\text{RaaiR} = \text{p-R-C}_6\text{H}_4\text{-N=N-C}_3\text{H}_2\text{-NN}$, abbreviated as *N,N'*-chelator, $\text{R} = \text{Me, Et, Bz, p-R}=\text{H, Me, Cl}$] were reacted with NaNO_2 (excess amount >2 mol) under stirring at 343-353 K in aqueous alcohol to give $[\text{Ru}(\text{NO}_2)(\text{RaaiR})(\text{tpy})]^+$ (**3a-3i**) in good yield (65-85%). The synthetic routes are shown below. The nitrites were synthesized in low yield either directly on stirring NaNO_2 in ethanol-acetone mixture for 30 h or in situ synthesis of the aquo complex by AgNO_3 followed by the reaction with NaNO_2 . The composition of the complexes is supported by microanalytical results. Room temperature solid state magnetic susceptibility measurements show that the complexes are diamagnetic. Trituration of solid $[\text{Ru}(\text{NO}_2)(\text{RaaiR})(\text{tpy})](\text{ClO}_4)$ in concentrated HClO_4 at ambient condition gives an orange-red solution from which the nitrosyl complexes $[\text{Ru}(\text{NO})(\text{RaaiR})(\text{tpy})](\text{ClO}_4)_3$ are isolated. In alkaline media nitrosyl complexes, regenerate the corresponding nitrite precursors (**3a-3i**). The reaction of H^+ with coordinated NO^+ group in nitrite complexes and the nucleophilic attack of OH^- on the NO in nitrosyls are the key steps for such reaction.



The violet nitrites are soluble in common organic solvents but insoluble in H_2O whereas the orange-red nitrosyls are soluble in H_2O and in a range of common organic solvents viz., methanol, ethanol, partly soluble in acetone, acetonitrile, chloroform, dichloromethane. In

MeCN, nitroso behave as 1:3 electrolytes ($\lambda = 160-190$ nm) whereas 1:1 electrolytic behaviour is found for type nitrite complexes ($\lambda = 60-90$ nm) as indicated by their very low λ_M values. Chemical oxidation of the aqua complex by excess aqueous ceric solution in 1 (N) H_2SO_4 leads to the spontaneous formation of a yellow colored oxo species and the process follow by oxidising the benzylic alcohol solution.

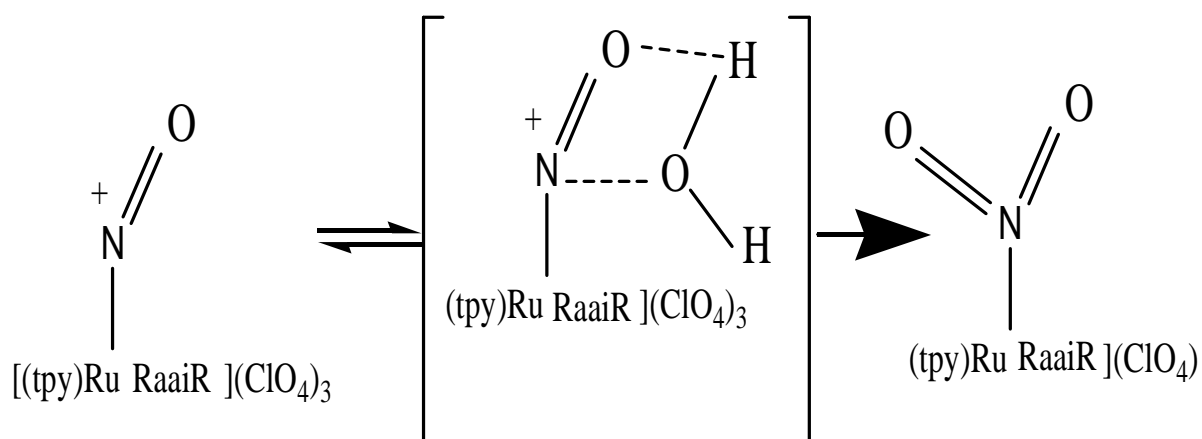


Spectral Studies

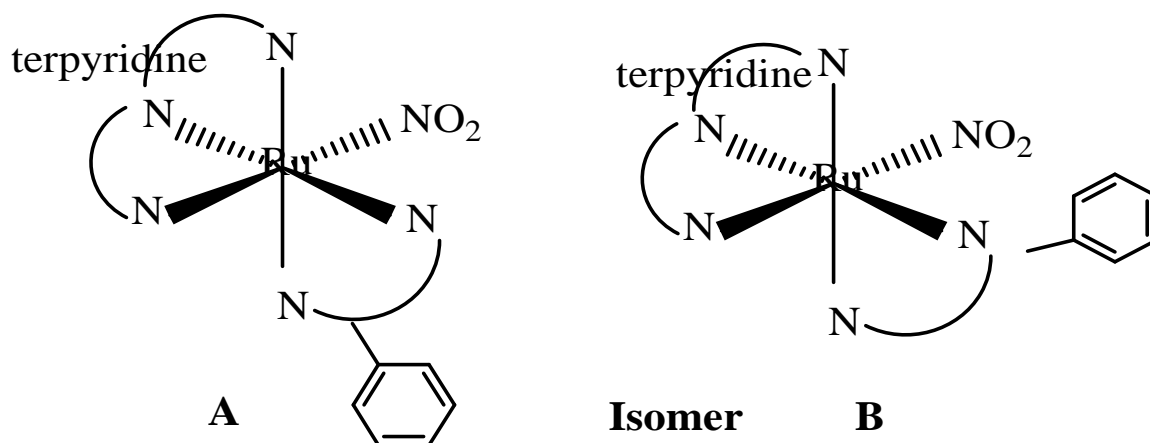
I.r. spectra of dinitro complexes, $[Ru(NO_2)(RaaiR)(tpy)]$ show a 1:1 correspondence to the spectra of the dichloro analogue, *ctc*- $[RuCl(RaaiR)(tpy)]$ except the appearance of intense stretching at 1300-1335 and 1250-1280 cm^{-1} with concomitant loss of $\nu(Ru-Cl)$ at 320-340 cm^{-1} . They are assigned as symmetric and asymmetric stretching of NO_2 i.e. $(NO_2)_{asym}$ and $(NO_2)_{sym}$, respectively (Fig. 1). The $\nu(N=N)$ and $\nu(C=N)$ appear at 1365-1380 and 1570-1600 cm^{-1} , respectively. Mono-nitroso-ruthenium(II), $[Ru(NO)(RaaiR)(tpy)](ClO_4)_2$ show a very strong stretch in the 1910-1925 cm^{-1} range which is conspicuously absent in the spectra of $[Ru(NO_2)(RaaiR)(tpy)]$. This is certainly due to the stretching mode of $\nu(NO)$ of the coordinated nitrosyl group. Nitric oxide formally acts as cationic donor (NO) and binds both in the linear and bent N-O fashion. The stretching frequency $\nu(NO)$ qualitatively determines the stereochemistry of M-N-O bonding (angle is nearly 180). Usually, $\nu(NO) > 1700$ cm^{-1} has been assigned to linear M-N-O bond. Thus, the present series of Ru-NO complexes are assumed to contain linear NO group. Other important frequencies are $\nu(HO)$ at 3350-3400 cm^{-1} and $\nu(ClO_4)$ at 1140-1145, 1110-1120 and 1080-1090 cm^{-1} along with weak bands at 640 and 625 cm^{-1} . Triplet splitting pattern of ClO may presumably be due to some sort of hydrogen bonding interaction, $Cl \cdots O \cdots H(O/C)$.

The solution electronic spectra of these new complexes were recorded in dry acetonitrile. The nitro complexes in MeCN showed three to four bands in the region 719–254 nm. All the complexes are diamagnetic, indicating the presence of ruthenium in the +2 oxidation state. The ground state of ruthenium(II) in an octahedral environment is $^1A_{1g}$, arising from the t_{2g}^6 configuration. The excited state terms are $^3T_{1g}$, $^3T_{2g}$, $^1T_{1g}$ and $^1T_{2g}$. Hence four bands corresponding to the transition $^1A_{1g} \rightarrow ^3T_{1g}$, $^1A_{1g} \rightarrow ^3T_{2g}$, $^1A_{1g} \rightarrow ^1T_{1g}$ and $^1A_{1g} \rightarrow ^1T_{2g}$ are possible in order of increasing energy. The electronic spectral bands at around 719–653 nm are assigned to $^1A_{1g} \rightarrow ^1T_{1g}$. The other high intensity band in the visible region around 504–519 nm has been assigned to charge transfer transitions arising from the metal t_{2g} level to the unfilled π^* molecular orbital of the ligand. The high intensity bands around 330–310 nm and

272–254 nm has been designated as $n\text{-}\pi^*$ and $\pi\text{-}\pi^*$ transitions respectively. The pattern of the electronic spectra for all the complexes indicate the presence of an octahedral environment around the ruthenium(II) ion similar to that of other ruthenium octahedral complexes.. The electronic spectrum of nitroso in an aqueous solution does not reveal the typical bands observed. These transitions are most probably shifted to much higher energy because of the strong stabilization of the metal d orbitals. The equivalent intraligand transitions involving RaaiR appear at higher energy, overlapping with the metal-to-ligand charge-transfer bands both are thus responsible for the high-intensity absorption in the UV region. Nitro complexes (**3a-3i**) exhibit multiple transitions in the uv-visible region. They display intense MLCT transition in the 550-560 nm range along with weak longer wavelength absorption near 750 nm (shoulder). In nitroso derivatives, $[\text{Ru}(\text{NO})(\text{RaaiR})(\text{tpy})](\text{ClO}_4)_3$ the intense absorption bands are further shifted to shorter wavelength, near 420 nm along with a weak band near 600 nm. This is attributed to strong $d(\text{Ru}) \rightarrow \pi^*(\text{NO})$ back bonding which stabilizes the d level and consequently shifts the MLCT band to the lower wavelength region. The nitrosyl complexes are found to be stable only in dry acetonitrile solution. In ordinary acetonitrile or in contact with moister the spectrum spontaneously changes and levels off with the spectrum of precursor dinitro derivative. The transformation has been proved through product isolation in one case, and characterized comparing of its properties with an authentic sample. The conversion from nitroso into the nitro complex is followed by the following mechanism.



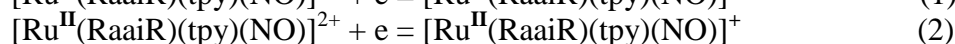
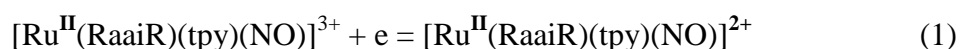
The ^1H n.m.r. spectra of $[\text{Ru}(\text{NO}_2)(\text{RaaiR})(\text{tpy})]$ (**3a-3i**) complexes were assigned on comparing with dichloro precursor (Table 1). The aryl protons (7-H—13-H) of (**3a-3i**) are downfield shifted by 0.1-0.07 ppm as compared to those of the parent dichloro derivatives. They are affected by substitution; 7,8- and 11,12-H are severely perturbed due to changes in the electronic properties of the substituents in the N- CH_3 -position. Imidazole 4- and 5-H appear as doublet at the lower frequency side of the spectra (7.0-7.2 ppm for 4-H; 6.9-7.1 ppm for 5-H). The aryl-Me (R = Me) in (**3a-3i**) appears as a single signal at 2.30 ppm and is in consonance with stereoretentive nucleophilic substitution during synthesis of dinitro complexes from dichloroparent complexes via aquo derivatives. The mononitrosyls, $[\text{Ru}(\text{NO})(\text{RaaiR})(\text{tpy})](\text{ClO}_4)_3$ exhibit similar pattern of signals in the aromatic portion and the spectra have been shifted to higher field by 0.03-0.15 ppm from those of respective dinitro derivatives. It is due to better $d(\text{Ru}) \rightarrow \pi^*(\text{NO})$ charge transfer which increases hardness of Ru(II) leading to strong π -interaction with the chelator. The solution ^1H NMR spectra support at least the presence of two isomers in different proportion.



Redox Properties

The potential values of the complexes in dry acetonitrile solution are measured (Fig. 1). The cyclic voltammogram of $[\text{Ru}(\text{NO}_2)(\text{RaaiR})(\text{tpy})](\text{ClO}_4)$ exhibit some unusual behaviour on repetitive cycles. The reduction sweep shows a new wave that has a counter oxidative wave on the second sweep. The first primary redox process ($E = 1.3\text{-}1.13\text{ V}$) is assigned to Ru(III)/Ru(II) couple. The nitrosyl complexes, $[\text{Ru}(\text{NO})(\text{RaaiR})(\text{tpy})](\text{ClO}_4)_3$ exhibit multiple redox responses in the potential range $+2.0\text{ V}$ to -2.0 V versus s.c.e. Two quasi-reversible reductive responses in the potential 0.5 to 0.6 V and -0.1 to -0.2 V are seen. The couples IV and V are assigned to successive one-electron reductions of the coordinated NO unit; [Ru-NO

Ru-NO (couple II), Ru-NO → Ru-NO (couple III)]. The couple III is irreversible, indicating instability of the reduced species. High potential voltammetric wave at $1.4\text{-}1.5\text{ V}$ (couple 1) ($E = 120\text{ mV}$) is assigned to the Ru(III)/Ru(II) couple. The azo group may accommodate two electrons and hence two coordinated ligands should exhibit four reductive responses. However, within the available potential window three reductions were clearly observable. The nitrosyl complexes display multiple redox processes in the experimental potential range (couples I–VI). At the positive side of the SCE they exhibit systematically one reversible reductive process near 0.5 V followed by another irreversible reduction near 0.1 V . The reduced species is found to be unstable even at 273 K , which has precluded its isolation and further studies. The first two reductions (couples II and III) are assigned to successive one-electron reductions of the coordinated NO unit, eqns. (1) and (2).



The reduction potential of $\text{Ru-NO}^+ \rightarrow \text{Ru-NO}$ [couple II, eqn. (1)] of nitroso-complexes is close to that of uncoordinated NO ($E = 0.74\text{ V}$). This reveals that the electrophilicity of the coordinated NO in the present set of complexes is comparable to that of free NO. The insignificant π interaction of NO in the present nitrosyl complexes is presumably the primary dictating factor for the observed high reduction potential. Although the first reduction process $\text{Ru-NO}^+ \rightarrow \text{Ru-NO}$ (couple II) is stable on the coulometric timescale, the second $\text{Ru-NO} \rightarrow \text{Ru-NO}^-$ is unstable even on cyclic voltammetric timescale. Nitrosyl complexes show one additional quasi-reversible oxidation process near 1.60 V . The oxidation process corresponding to it may be assigned to the ruthenium(II)–ruthenium(III) oxidation as all other redox active centres in the complex moiety are only susceptible to reduction. The nitro as well as nitroso complexes display three additional successive one-electron reductions to negative potentials of the SCE. Since both coordinated ligands are known to accept successively two electrons in their lowest unoccupied molecular orbitals, the observed reductions are

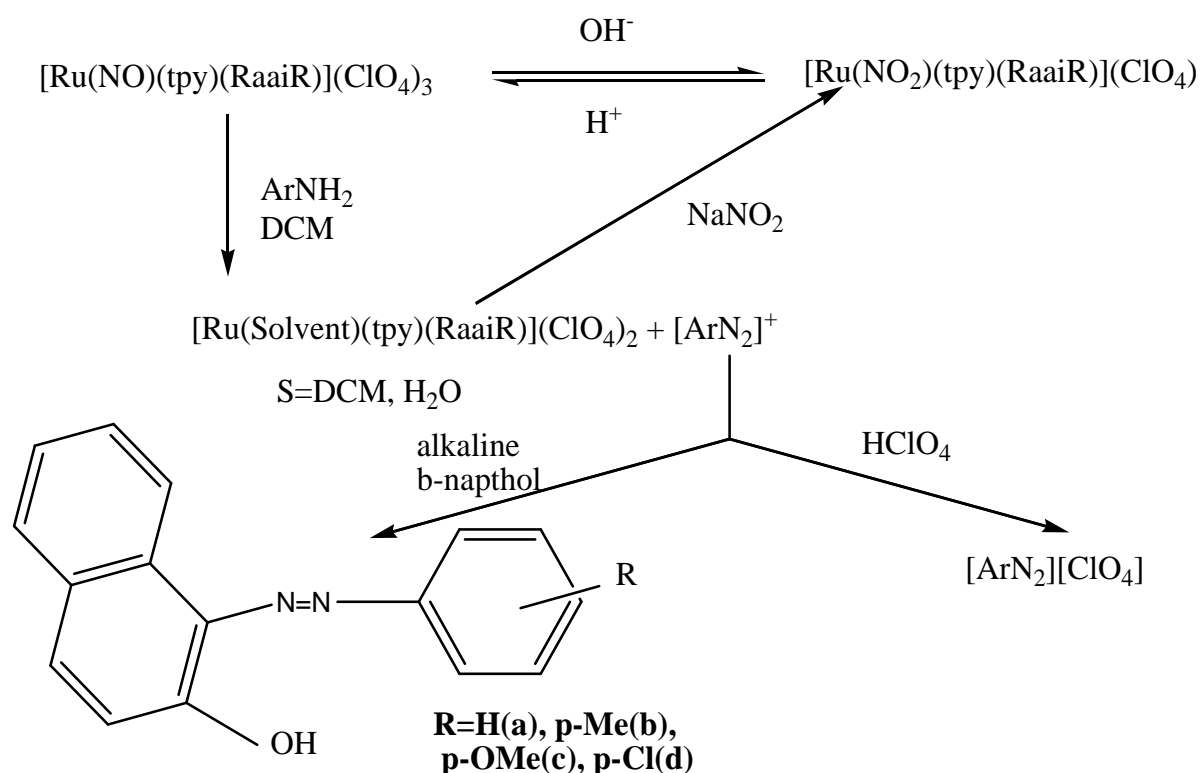
considered to be ligand based processes. Electrochemical oxidations of complexes in acetonitrile solvent at 1.5 V *versus* SCE develop unstable orange oxidised species. The oxidised complexes display voltammograms which are identical to those of the starting bivalent complexes. They exhibit one intense LMCT transition in the visible region and intra-ligand transitions in the UV region.

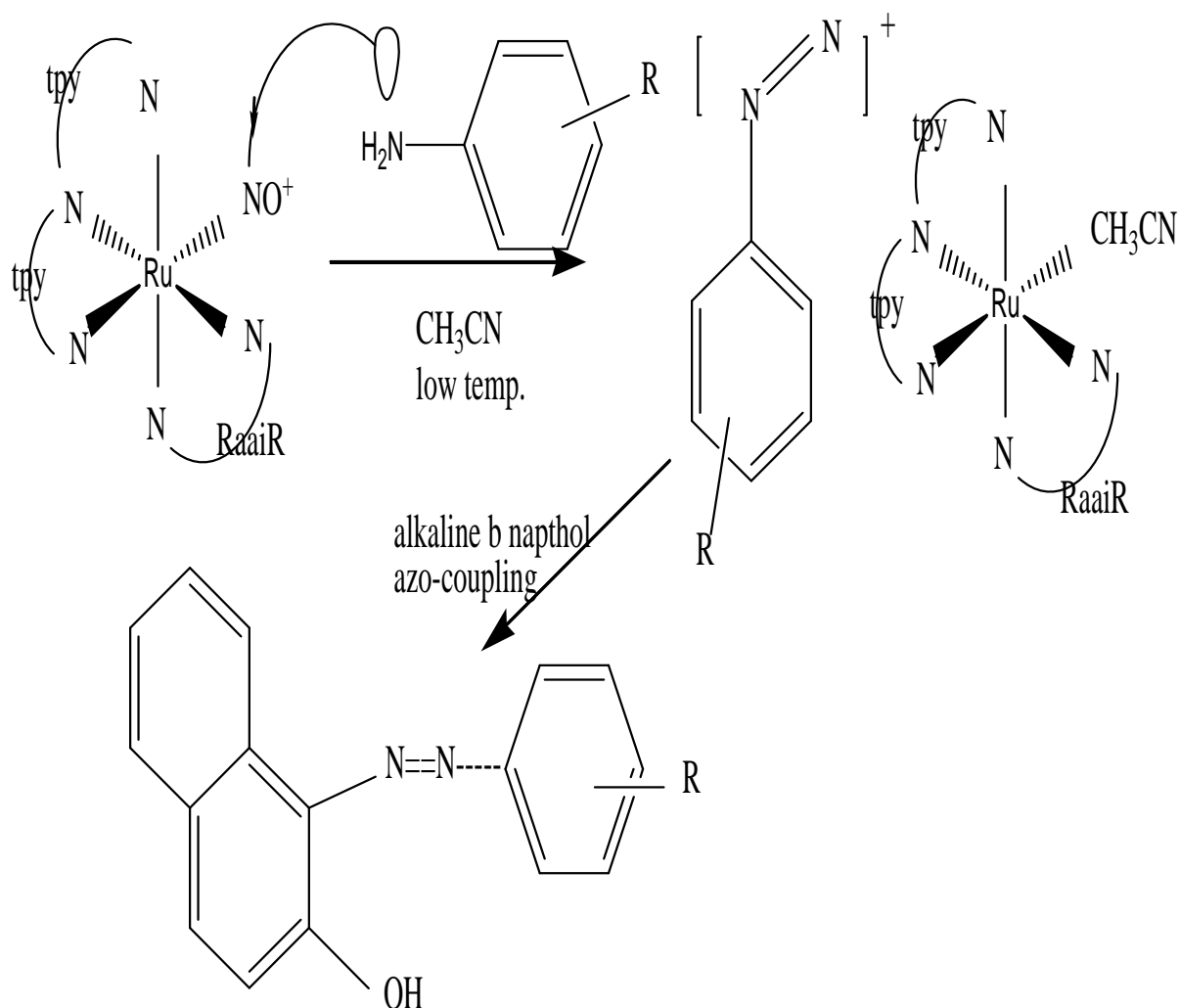
Spectroelectrochemical Correlation

Nitro complexes display the lowest MLCT transition of the type $t_2(\text{Ru})$ to Ligand LUMO near 500 nm. The quasi-reversible Ru(III)/Ru(II) couple lies in the 1.10–1.4 V range, and the first ligand reduction in the range -0.45–0.67 V (one electron). The energy of the above band can be predicted from the experimentally observed electrochemical data. There is a linear relationship between the t_{MLCT} and DE.

Reactivity Study

Reaction of the mononitrosyl complexes with primary amines were studied by the following sequence. To investigate the reaction mechanism it was studied in two solvents, in acetonitrile and in dichloromethane. This monoquo complex produces the monoacetonitrile complex on treatment with acetonitrile. One real advantage of such reaction is the possibility of developing analytical route for synthetic nitrosation of organic substrate using $[\text{Ru}(\text{NO})(\text{RaaiMe})(\text{tpy})](\text{ClO}_4)_3$ as the source of NO under mildly acidic condition.





In conclusion, nitro complexes of ruthenium (II)–azoimidazole, [Ru(NO₂)(RaaiR)(tpy)] have been synthesised by stereoretentive reaction of aquo complex [Ru(OH₂)(RaaiR)(tpy)] with nitrite ion. The complexes exhibit strong MLCT transitions. Voltammetric study shows Ru(III)/Ru(II) couple along with successive ligand-based reductions and additionally NO⁺ reductions in nitrosyl derivatives. The electrophilic activity of bound NO has been established through diazotization of ArNH₂.

ACKNOWLEDGEMENT

Department of Science and Technology (DST) is thanked for financial support. (FAST TRACK Grand No. SERB/F/4888/2012-13 Dated 30.11.2012. Project Title: Gold(I) & Gold(III) Arylazoimidazole (N, N Donor) & Oxo Complexes : Synthesis, Structure, Spectral Study, Electrochemistry And Chemical Reactivity).

REFERENCE

- Abrahamsson, M., M.J. Lundqvist, H. Wolpher, O. Johansson, L. Eriksson, J. Bergquist, T. Rasmussen, H.C. Becker, L. Hammarström, P.O. Norrby, B. Åkermark and P. Persson. 2008. Steric Influence on the Excited-State Lifetimes of Ruthenium Complexes with Bipyridyl–Alkanylene–Pyridyl Ligands, *Inorg. Chem.* 47(9):3540–3548. DOI: 10.1021/ic7019457.

- Alary, F., M.B. Pasqua, J.L. Heully, C.J. Marsden and P. Vicendo. 2008. Theoretical Characterization of the Lowest Triplet Excited States of the Tris-(1,4,5,8-tetraazaphenanthrene) Ruthenium Dication Complex. *Inorg. Chem.* 47(12):5259–5266. DOI: 10.1021/ic800246t.
- Almodares, Z., S.J. Lucas, B.D. Crossley, A.M. Basri, C.M. Pask, A.J. Hebden, R.M. Phillips, and P.C. McGowan. 2014. Rhodium, Iridium, and Ruthenium Half-Sandwich Picolinamide Complexes as Anticancer Agents. *Inorg. Chem.* 53(2):727–736. DOI: 10.1021/ic401529u.
- Alós, J., T. Bolaño, M.A. Esteruelas, M. Oliván, E. Oñate, and M. Valencia. 2014. POP–Pincer Ruthenium Complexes: d^6 Counterparts of Osmium d^4 Species. *Inorg. Chem.* 53(2):1195–1209. DOI: 10.1021/ic402795g.
- Al-Rawashdeh, N.A.F., S. Chatterjee, J.A. Krause, and W. B. Connick. 2013. Ruthenium Bis-diimine Complexes with a Chelating Thioether Ligand: Delineating 1,10-Phenanthrolyl and 2,2-Bipyridyl Ligand Substituent Effects. *Inorg. Chem.* 53(1):294–307. DOI: 10.1021/ic4022454.
- Cheung, W.M., H.Y. Ng, I.D. Williams and W.H. Leung. 2008. Ruthenium Complexes with Tetraphenylimidodiphosphinate: Syntheses, Structures, and Applications to Catalytic Organic Oxidation. *Inorg. Chem.* 47(10):4383–4391. DOI: 10.1021/ic800018d
- Cui, Y., Y.L. Niu, M. Li Cao, K. Wang, H. Jun Mo, Y. Rui Zhong and BHui Ye. 2008. Ruthenium(II) 2,2-Bibenzimidazole Complex as a Second-Sphere Receptor for Anions Interaction and Colorimeter. *Inorg. Chem.* 47(13):5616–5624. DOI: 10.1021/ic702050b
- Doro, F.G., E.E. Castellano, L.A.B. Moraes, M.N. Eberlin and E. Tfouni. 2008. Cyclam 4 to 3 Ligand Denticity Change Upon Mono-N-Substitution with a Carboxypropyl Pendant Arm in a Ruthenium Nitrosyl Complex. *Inorg. Chem.* 47(10):4118–4125. DOI: 10.1021/ic702078p.
- Fiore, G.L., B.N. Goguen, J.L. Klinkenberg, S.J. Payne, J.N. Demas, and C.L. Fraser. 2008. Ruthenium Tris(bipyridine) Complexes with Sulfur Substituents: Model Studies for PEG Coupling. *Inorg. Chem.* 47(14): 6532–6540. DOI: 10.1021/ic800262d.
- Garza-Ortiz, A., P. Uma Maheswari, M. Siegler, A.L. Spek and J. Reedijk. 2008. Ruthenium(III) Chloride Complex with a Tridentate Bis(arylimino)pyridine Ligand: Synthesis, Spectra, X-ray Structure, 9-Ethylguanine Binding Pattern, and In Vitro Cytotoxicity. *Inorg. Chem.* 47(15):6964–6973. DOI: 10.1021/ic8005579.
- Gkionis, K., J.A. Platts and J.G. Hill. 2008. Insights into DNA Binding of Ruthenium Arene Complexes: Role of Hydrogen Bonding and Stacking. *Inorg. Chem.* 47 (9):3893–3902. DOI: 10.1021/ic702459h.
- Hamelin, O., S. Ménage, F. Charnay, M. Chavarot, J.L. Pierre, J. Pécaut, and M. Fontecave. 2008. New Polydentate Ligand and Catalytic Properties of the Corresponding Ruthenium Complex During Sulfoxidation and Alkene Epoxidation. *Inorg. Chem.* 47(14):6413–6420. DOI: 10.1021/ic800534v.
- Hesp, K.D., M.A. Rankin, R. McDonald and M. Stradiotto. 2008. Synthesis and Characterization of a Cationic Ruthenium Complex Featuring an Unusual Bis(2 -BH) Monoborane Ligand. *Inorg. Chem.* 47(17):7471–7473. DOI: 10.1021/ic801300m.
- Hurst, J.K., J.L. Cape, A.E. Clark, S. Das and C. Qin. 2008. Mechanisms of Water Oxidation Catalyzed by Ruthenium Diimine Complexes, *Inorg. Chem.* 47(6):1753–1764. DOI: 10.1021/ic700724h.
- Johansson, O. and R. Lomoth. 2008. Molecular Hysteresis in a Rigid Dinuclear Ruthenium Polypyridyl Complex Incorporating a Ligand-Bound Ambidentate Motif. *Inorg. Chem.* 47(13):5531–5533. DOI: 10.1021/ic800075b.
- Karlsson, S., J. Modin, H.C. Becker, L. Hammarström and H. Grennberg. 2008. How Close Can You Get? Studies of Ultrafast Light-Induced Processes in Ruthenium-[60] Fullerene Dyads with Short Pyrazolino and Pyrrolidino Links. *Inorg. Chem.* 47(16):7286–7294. DOI: 10.1021/ic800168d.
- Kobayashi, A., T. Ohba, E. Saitoh, Y. Suzuki, S. Noro, H.C. Chang, and M. Kato. 2014. Flexible Coordination Polymers Composed of Luminescent Ruthenium(II) Metalloligands: Importance of the Position of the Coordination Site in Metalloligands. *Inorg. Chem.* Articles ASAP (As Soon As Publishable), Publication Date (Web): February 21, 2014 (ArticleDOI: 10.1021/ic402683j).
- Man, W.L., H.K. Kwong, W.W.Y. Lam, J. Xiang. 2008. Tsz-Wing Wong, Wing-Hong Lam, Wing-Tak Wong, Shie-Ming Peng and Tai-Chu Lau, General Synthesis of (Salen)ruthenium(III) Complexes via N...N Coupling of (Salen)ruthenium(VI) Nitrides. *Inorg. Chem.* 47(13):5936–5944. DOI: 10.1021/ic800263n.
- Mulcahy, S.P., S. Li, R. Korn, X. Xie and E. Meggers. 2008. Solid-Phase Synthesis of Tris-heteroleptic Ruthenium(II) Complexes and Application to Acetylcholinesterase Inhibition. *Inorg. Chem.* 47(12):5030–5032. DOI: 10.1021/ic800080b.

- Neill, J., A.S. Nam, K.M. Barley, B. Meza and D.N. Blauch. 2008. Redox Transformations of Bis(2,2'-bipyridine)(1-methyl-1-pyridin-2-yl-ethylamine)ruthenium(II). *Inorg. Chem.* 47(12):5314–5323. DOI: 10.1021/ic800483g.
- Norris, M.R., J.J. Concepcion, C.R.K. Glasson, Z. Fang, A.M. Lapedes, D.L. Ashford, J.L. Templeton, and T.J. Meyer. 2013. Synthesis of Phosphonic Acid Derivatized Bipyridine Ligands and Their Ruthenium Complexes. *Inorg. Chem.* 52(21):12492–12501. DOI: 10.1021/ic4014976.
- Odongo, O.S., M.J. Heeg, Y.J. Chen, P. Xie and J.F. Endicott. 2008. Effects of Excited State–Excited State Configurational Mixing on Emission Bandshape Variations in Ruthenium–Bipyridine Complexes. *Inorg. Chem.* 47(17):7493–7511. DOI: 10.1021/ic7024473.
- Pal, A.K., S. Nag, J.G. Ferreira, V. Brochery, G. La Ganga, A. Santoro, S. Serroni, S. Campagna, and G.S. Hanan. 2014. Red-Emitting [Ru(bpy)₂(N-N)]²⁺ Photosensitizers: Emission from a Ruthenium(II) to 2,2'-Bipyridine ³MLCT State in the Presence of Neutral Ancillary “Super Donor” Ligands. *Inorg. Chem.* 53(3):1679–1689. DOI: 10.1021/ic4028332.
- Patra, S.C., T. Weyhermüller, and P. Ghosh. 2014. Ruthenium, Rhodium, Osmium, and Iridium Complexes of Osazones (Osazones = Bis-Arylhydrazones of Glyoxal): Radical versus Nonradical States. *Inorg. Chem.* 53(5):2427–2440. DOI: 10.1021/ic4022432.
- Rathgeb, A., A. Böhm, M.S. Novak, A. Gavriluta, O. Dömötör, J.B. Tommasino, É.A. Enyedy, S.Shova, S. Meier, M.A. Jakupc, D. Luneau, and V.B. Arion. 2014. Ruthenium-Nitrosyl Complexes with Glycine, l-Alanine, l-Valine, l-Proline, d-Proline, l-Serine, l-Threonine, and l-Tyrosine: Synthesis, X-ray Diffraction Structures, Spectroscopic and Electrochemical Properties, and Antiproliferative Activity. *Inorg. Chem.* 53(5):2718–2729. DOI: 10.1021/ic4031359.
- Rebouças, J.S., E.L.S. Cheu, C.J. Ware, B.R. James and K.A. Skov. 2008. Synthetic and Mechanistic Aspects of a New Method for Ruthenium-Metalation of Porphyrins and Schiff-Bases. *Inorg. Chem.* 47(17):7894–7907. DOI: 10.1021/ic800616q.
- Saha, S. and B. Captain. 2014. Synthesis and Structural Characterization of Ruthenium Carbonyl Cluster Complexes Containing Platinum with a Bulky N-Heterocyclic Carbene Ligand. *Inorg. Chem.* 53(2):1210–1216. DOI: 10.1021/ic402832b
- Singh, P., A. Kumar Das, B. Sarkar, M. Niemeyer, Fe. Roncaroli, J.A. Olabe, J. Fiedler, S. Zális and W. Kaim. 2008. Redox Properties of Ruthenium Nitrosyl Porphyrin Complexes with Different Axial Ligation: Structural, Spectroelectrochemical (IR, UV–Visible, and EPR), and Theoretical Studies. *Inorg. Chem.* 47(16):7106–7113. DOI: 10.1021/ic702371t.
- Sinn, S., B. Schulze, C. Friebe, D.G. Brown, M. Jäger, E. Altunta, J. Kübel, O. Guntner, C.P. Berlinguette, B. Dietzek, and U.S. Schubert. 2014. Physicochemical Analysis of Ruthenium(II) Sensitizers of 1,2,3-Triazole-Derived Mesoionic Carbene and Cyclometalating Ligands. *Inorg. Chem.* 53(4):2083–2095. DOI: 10.1021/ic402702z.
- Sinn, S., B. Schulze, C. Friebe, D.G. Brown, M. Jäger, J. Kübel, B. Dietzek, C.P. Berlinguette, and U.S. Schubert. 2014. A Heteroleptic Bis (tridentate) Ruthenium(II) Platform Featuring an Anionic 1,2,3-Triazolate-Based Ligand for Application in the Dye-Sensitized Solar Cell. *Inorg. Chem.* 53(3):1637–1645. DOI: 10.1021/ic402701v.
- Smart, K.A., M. Grellier, Y. Coppel, L. Vendier, S.A. Mason, S.C. Capelli, A. Albinati, V. Montiel-Palma, M.A. Muñoz-Hernández, and S. Sabo-Etienne. 2014. Nature of Si–H Interactions in a Series of Ruthenium Silazane Complexes Using Multinuclear Solid-State NMR and Neutron Diffraction. *Inorg. Chem.* 53(2):1156–1165. DOI: 10.1021/ic4027199.
- Staehele, R., L. Tong, L. Wang, L. Duan, A. Fischer, M.S.G. Ahlquist, L. Sun, and S. Rau. 2014. Water Oxidation Catalyzed by Mononuclear Ruthenium Complexes with a 2,2'-Bipyridine-6,6'-dicarboxylate (bda) Ligand: How Ligand Environment Influences the Catalytic Behavior. *Inorg. Chem.* 53(3):1307–1319. DOI: 10.1021/ic401701z.
- Staniszewski, A., W.B. Heuer and G.J. Meyer. 2008. High-Extinction Ruthenium Compounds for Sunlight Harvesting and Hole Transport. *Inorg. Chem.* 47(16):7062–7064. DOI: 10.1021/ic800171h.
- Su, W., Q. Qian, P. Li, X. Lei, Q. Xiao, S. Huang, C. Huang, and J. Cui. 2013. Synthesis, Characterization, and Anticancer Activity of a Series of Ketone-N⁴-Substituted Thiosemicarbazones and Their Ruthenium(II) Arene Complexes. *Inorg. Chem.* 52(21):12440–12449. DOI: 10.1021/ic401362s.
- Tommaso, D.D., S.A. French, A.Z. Gerosa, F. Hancock, E.J. Palin and C. Richard A. Catlow. 2008. Computational Study of the Factors Controlling Enantioselectivity in Ruthenium(II) Hydrogenation Catalysts. *Inorg. Chem.* 47(7):2674–2687. DOI: 10.1021/ic701981v.
- Werrett, M.V., S. Muzzioli, P.J. Wright, A. Palazzi, P. Raiteri, S. Zacchini, M. Massi, and S. Stagni. 2014. Proton-Induced Reversible Modulation of the Luminescent Output of

- Rhenium(I), Iridium(III), and Ruthenium(II) Tetrazolate Complexes. *Inorg. Chem.* 53(1):229–243. DOI: 10.1021/ic402187e.
- Whittington, C.L., L. Wojtas, and R.W. Larsen. 2013. Ruthenium(II) Tris(2,2-bipyridine)-Templated Zinc(II) 1,3,5-Tris(4-carboxyphenyl)benzene Metal Organic Frameworks: Structural Characterization and Photophysical Properties. *Inorg. Chem.* 53(1). DOI: 10.1021/ic402614w.
- Younes, A.H. and T.H. Ghaddar. 2008. Synthesis and Photophysical Properties of Ruthenium-Based Dendrimers and Their Use in Dye Sensitized Solar Cells. *Inorg. Chem.* 47(8):3408–3414. DOI: 10.1021/ic702432u.
- Zhou, R., B. Sedai, G.F. Manbeck, and K.J. Brewer. New Supramolecular Structural Motif Coupling a Ruthenium(II) Polyazine Light Absorber to a Rhodium(I) Center. *Inorg. Chem.* 52 (23):13314–13324. DOI: 10.1021/ic4006828.